Developmental and Comparative Immunology 151 (2024) 105106

Contents lists available at ScienceDirect

Developmental and Comparative Immunology

journal homepage: www.elsevier.com/locate/devcompimm

Peripheral inflammation-induced changes in songbird brain gene expression: 3' mRNA transcriptomic approach

Nithya Kuttiyarthu Veetil [a], Haniel Cedraz de Oliveira [b,c], Mercedes Gomez-Samblas [a,d], Daniel Divín [a], Balraj Melepat [a], Eleni Voukali [a], Zuzana Świderská [a], Tereza Krajzingrová [a], Martin Těšický [a], Ferris Jung [e], Vladimír Beneš [e], Ole Madsen [b], Michal Vinkler [a,*]

[a] Charles University, Faculty of Science, Department of Zoology, Viničná 7, 128 43, Prague, Czech Republic
[b] Wageningen University and Research, Department of Animal Sciences, Animal Breeding and Genomics, Droevendaalsesteeg 1, 6708PB, Wageningen, the Netherlands
[c] Federal University of Viçosa, Viçosa, MG, 36570-900, Brazil
[d] Granada University, Science faculty, Department of Parasitology, CP:18071, Granada, Granada, Spain
[e] EMBL, Genomics Core Facility, Meyerhofstraße 1, 69117, Heidelberg, Germany

ARTICLE INFO

Keywords:
Neuroimmune interaction
Avian cytokine
Differential gene expression
Neurogenic inflammation
Peripheral immunity
Transcriptome

ABSTRACT

Species-specific neural inflammation can be induced by profound immune signalling from periphery to brain. Recent advances in transcriptomics offer cost-effective approaches to study this regulation. In a population of captive zebra finch (*Taeniopygia guttata*), we compare the differential gene expression patterns in lipopolysaccharide (LPS)-triggered peripheral inflammation revealed by RNA-seq and QuantSeq. The RNA-seq approach identified more differentially expressed genes but failed to detect any inflammatory markers. In contrast, QuantSeq results identified specific expression changes in the genes regulating inflammation. Next, we adopted QuantSeq to relate peripheral and brain transcriptomes. We identified subtle changes in the brain gene expression during the peripheral inflammation (e.g. up-regulation in *AVD-like* and *ACOD1* expression) and detected co-structure between the peripheral and brain inflammation. Our results suggest benefits of the 3′end transcriptomics for association studies between peripheral and neural inflammation in genetically heterogeneous models and identify potential targets for the future brain research in birds.

1. Introduction

Inflammation in brain is often linked with serious behavioural changes and health disorders (Kempuraj et al., 2017). In humans, the outcomes of mild neuroinflammation affect behaviour and psychiatric state, including development of clinical depression (Brites and Fernandes, 2015; DiSabato et al., 2016; Yoshino et al., 2021). In rodents, anxiety and depression-like behaviour can be triggered by stimulation of inflammation in the periphery (Bluthé et al., 1994; Mayerhofer et al., 2017; Painsipp et al., 2010; Sulakhiya et al., 2016). During inflammation, profound immune signalling from periphery to the central nervous system (CNS) can induce neuroinflammation (Danielski et al., 2018; Hernández-Romero et al., 2012). Important roles in this regulation are played by soluble signalling molecules, pro-inflammatory cytokines (e.g. interleukin 1 β, *IL1B* (Lopez-Castejon and Brough, 2011); produced by stimulated peripheral leukocytes that cross the blood brain barrier, stimulate microglia and astrocytes and induce neuroinflammation (Becher et al., 2017; Erickson et al., 2012). While recent evidence suggests interspecific differences in this regulation (Divín et al., 2022), presently we are not sure how common this phenomenon is across vertebrates. Except for humans and rodents in which research of neuroinflammation is widespread, only few studies describe this phenomenon in chickens (Asfor et al., 2021; Du et al., 2020; Song et al., 2020; Zeng et al., 2019) and data from other taxa are sparse (Scalf et al., 2019).

Across vertebrates, variability is observed in peripheral immune responses, contributing to variation in susceptibility to infections (Seal et al., 2021; Vinkler et al., 2023; Zheng et al., 2020). Much of this variation is adaptive, diversified and shaped by natural selection acting across species and populations (Eskew et al., 2021; Minias and Vinkler,

* Corresponding author.
E-mail addresses: kuttiyan@natur.cuni.cz (N. Kuttiyarthu Veetil), hanielcedraz@gmail.com (H. Cedraz de Oliveira), gomezsama@natur.cuni.cz (M. Gomez-Samblas), daniel.divin@natur.cuni.cz (D. Divín), melepatb@natur.cuni.cz (B. Melepat), voukalie@natur.cuni.cz (E. Voukali), zana.bain@gmail.com (Z. Świderská), t.krajzingrova@gmail.com (T. Krajzingrová), martin.tesicky@natur.cuni.cz (M. Těšický), fjung@embl.de (F. Jung), benes@embl.de (V. Beneš), ole.madsen@wur.nl (O. Madsen), michal.vinkler@natur.cuni.cz (M. Vinkler).

https://doi.org/10.1016/j.dci.2023.105106
Received 4 August 2023; Received in revised form 3 November 2023; Accepted 21 November 2023
Available online 25 November 2023

Abbreviations

BAQCOM – Bioinformatics Analysis for Quality Control and Mapping
CIA – Co-Inertia multivariate Analysis
DEG – Differentially Expressed Genes
DGE – Differential Gene Expression
GATK – Genome Analysis Toolkit
LPS – Lipopolysaccharide
RS – RNA-seq dataset
PCA – Principal Component Analysis
QS – QuantSeq dataset
RIN – RNA Integrity Number
RT-qPCR – Reverse transcription quantitative real-time PCR

2022; Peralta-Sánchez et al., 2012; Těšický et al., 2020). Model organisms often provide genetic uniformity that meets the research needs in controlled laboratory experiments but they lack the inter-individual variation observed in nature (Russell et al., 2017). While much is presently known about regulation of local and systemic inflammation in humans and laboratory rodents, little information is available to other species and especially birds, which represent an evolutionary parallel to mammals (Vinkler et al., 2022). Studies in new model species can provide novel insights into general mechanisms underlying immunity regulation and its interaction with other biological systems (Russell et al., 2017).

Avian-oriented research could become highly informative for the current understanding of neuroimmunology (Bramley et al., 2016). Birds show high neuronal densities and developed cognitive skills, comparable to mammals of much larger body mass (Olkowicz et al., 2016). However, majority of the research in avian neuroimmunology has so far been focused at the domestic chicken (*Gallus domesticus*) as a key model (Flores-Santin and Burggren, 2021; International Chicken Genome Sequencing Consortium, 2004). In chickens, the neuronal structures and cognitive skills are less developed than in other evolutionarily derived birds (Kverková et al., 2022), such as the passerines representing the majority of the extant avian species (Arnaiz-Villena et al., 2010; Hellgren and Ekblom, 2010; Romanov et al., 2014). Passerines share a number of cognitive and physiological adaptations convergent to primates. They mastered the vocal learning, which is linked to changes in brain structures analogous to humans (Aamodt et al., 2020). These birds also display memory-dependent behaviour associated with visual identification of food items, and often live in social groups like the primates, but are easier to handle and breed faster (Balakrishnan et al., 2010; Mello, 2014). Zebra finch (*Taeniopygia guttata*) is a recently emerged songbird model for immunological (Batra et al., 2020; Lopes et al., 2012; Mishra et al., 2019; Pedersen et al., 2017; Poole and Kitchen, 2022; Vinkler et al., 2022) and neurobehavioral research (Spierings and ten Cate, 2016), to which much information on the regulation of neuroimmune pathways is still missing (David et al., 2011). Furthermore, it has a fully sequenced high-quality genome and gene annotation (Warren et al., 2010), making it a suitable model for transcriptomic investigation.

Transcriptomics is a powerful approach for identification of key pathway-activation markers in non-model species. Several advancements in RNA sequencing have recently made transcript detection more precise (Hong et al., 2020; Ozsolak and Milos, 2011; Satam et al., 2023). Full-length RNA transcriptomics (RNA-seq) helps to precisely quantify the gene expression levels, assemble the sequences of new transcripts and understand alternative RNA processing (Ramsköld et al., 2012; Finotello and Di Camillo, 2015). Previously, the RNA-seq approach has provided relevant insights on gene expression changes during neuroinflammation and associated diseases in mice and humans (Canchi et al., 2020; Pulido-Salgado et al., 2018). However, RNA-seq approach requires deep sequencing and accurate standardisation of the library preparation procedures since otherwise bias can emerge from fragmentation and library construction steps, altering transcript representation and resulting in more enriched differentially expressed genes (DEGs) for longer transcripts than for the shorter ones (Wang et al., 2009). Furthermore, in cases of less common model species with substantially high inter-individual variation in immune responsiveness, RNA-seq requires investigation of high number of experimental subjects even for relatively simple experimental designs. Hence, despite the falling costs of sequencing, the sample size still can represent a limitation, urging for innovations in library processing, sequencing strategy and data analysis (Moll et al., 2014). To describe the general expression patterns of genes in the transcriptome, full-length sequence RNA-seq can represent an unnecessary investment. New 3' RNA-seq methods, such as QuantSeq, were designed to reduce the costs of general gene expression analysis (Jarvis et al., 2020; Moll et al., 2014), allowing comparing expression patterns across larger sets of samples. The QuantSeq, uses a protocol without any prior poly(A) enrichment or rRNA depletion, in which total RNA is not fragmented before reverse transcription and only single read per transcript is obtained (Ma et al., 2019), sequencing the RNA string close to its 3′ end (generally from the last exon and/or the 3′ untranslated region). Thus, in QuantSeq the number of reads mapped to a given transcript sequence is fully proportional to its expression (Corley et al., 2019).

The main objective of our study was to explore neural inflammation patterns of gene expression in zebra finch after stimulation of mild peripheral sterile inflammation triggered with bacterial lipopolysaccharide (LPS). Despite previous rich transcriptomic research conducted in the zebra finch brain, earlier research focused mostly on variation in gene expression of specific genes (e.g. MHC; Ekblom et al., 2010), transcriptomics of parental care (Kumari et al., 2022) and especially sex- (Friedrich et al., 2022; He et al., 2022) and species-specific (Pfenning et al., 2014) differences in gene expression related to vocal learning. Limited research has been so far conducted in passerine brain immunotranscriptomics (but see e.g. Scalf et al., 2019). First, we investigated the peripheral and systemic effects of our immune manipulation. Since previous studies in avian ecophysiology considered skin as a tissue of interest (Santiago-Quesada et al., 2015; Vinkler et al., 2010, 2012) that is also suitable for the investigation of the regulatory interconnection between the peripheral and systemic immune responses (Arck et al., 2006; Chen and Lyga, 2014; Paus et al., 2006; Peters et al., 2005), we started with analysis of the inflammation effects in skin. We adopted the classical Illumina RNA-seq method from the number of individuals equivalent to similar studies performed in lab mice (Crowell et al., 2020; Liu et al., 2021). Obtaining compromised results (likely due to inter-individual variation in immune responsiveness), we then adopted the QuantSeq approach that is applicable to an enlarged data set. Decreasing the per sample sequencing cost, we doubled the size of our transcriptomic data set. Here we report comparison of results from the two approaches, RNA-seq and QuantSeq. Next, we used the QuantSeq method for brain tissue transcriptomics to reveal the effects of our LPS treatment on gene expression changes in avian brain. Finally, we verified our key results through reverse transcription quantitative polymerase chain reaction (RT-qPCR) analysis.

2. Materials and methods

2.1. Experimental design

Twenty-four adult zebra finch males healthy in appearance were purchased from local hobby breeders (November 2018) and were immediately transported into the animal facility of the Faculty of Science, Charles University, Czech Republic, EU. For each individual, the body weight and tarsus length were measured. For this research, we selected only males, because of the known transcriptomic differences

between the sexes (Friedrich et al., 2022) and the need to limit the overall biological heterogeneity of our experimental sample. The birds were marked with coloured aluminium rings with ID codes and housed in two large aviaries where they were fed with millet and received tap drinking water *ad libitum*. The birds were kept for 3 days in quarantine under regular conditions (D12:N12, 22 °C). Before any manipulation, the magnitude of the tissue of the left wing-web (patagium) was measured in each bird three times with accuracy to 0.01 mm (Vinkler et al., 2010, 2012), using a thickness gage (Mitutoyo, Sakado, Japan, Cat. No. 547-312S). For the experiment, the 24 individuals were divided into two equally sized groups: 12 individuals represented unstimulated controls and 12 immune-stimulated treatments (for dataset details see Table S1 in Electronic Supplementary Material 1, ESM1). All treatment individuals received intraabdominal injection of 0.1 mg *Escherichia coli* LPS O55:B5 (product No. L2880, Sigma-Aldrich, St. Louis, Missouri, USA) dissolved in 100 μl Dulbecco's phosphate-buffered saline (product No. D5652, Sigma-Aldrich). Furthermore, the treatment birds also received an injection of 0.1 mg LPS O55:B5 (Abou Elazab et al., 2022; Casebere et al., 2015) dissolved in 20 μl sterile DPBS administrated subcutaneously into the left wing web (patagium) for testing the local inflammatory response (Wegmann et al., 2015). The experimental manipulations were performed in two consecutive days (two batches of 14 and 10 birds, both containing equal proportions of treatments and controls i.e. in the first batch 7 LPS-treated and 7 control birds, in the second batch 5 LPS-treated and 5 control birds). The LPS-treated birds and no-treatment controls were manipulated in the same way to experience similar levels of the handling stress. For each bird the stimulation period was individually set to 24 h (± 1 h), a period of assumed peripheral inflammation peak (Adelman et al., 2013) after which a second metrical tissue-magnitude measurement was taken from both the left and right patagium (again three times) and then each bird was euthanized by decapitation (Scalf et al., 2019; Vinkler et al., 2018). The research was approved by the Ethical Committee of Charles University, Faculty of Science (permits 13882/2011-30) and was carried out in accordance with the current laws of the Czech Republic and the European Union.

After the post-mortem blood collection from carotids (immediately after decapitation, using sodium heparin to prevent blood coagulation), blood smears were made by spreading a drop of blood over a glass slide. Selected tissues were immediately collected into RNAlater (Cat. No. R0901, Sigma-Aldrich), including brain hyperpallium (ca. 24 mm^3) and skin tissue necropsies from the patagium (wing web, area of ca. 6 mm^2, containing a layer of the skin tissue and associated leukocyte infiltrate). The total dissection time for each bird was <20 min. The collected tissues were immediately placed into the RNAlater, stored at +4 °C overnight and then frozen at −80 °C until analysis. The wing swelling score was later calculated as the average tissue thickness of the left wing after stimulation minus the average thickness of the right wing.

2.2. RNA isolation and sequencing

The brain and skin tissues were homogenized in 2 ml hard tissue homogenizing tubes containing beads (Cat. No: 19-628D, OMNI International, Kennesaw, GA, USA) using MagnaLyser (Cat. No. 41984075, Roche, Basel, Switzerland) and the total RNA was extracted by High Pure RNA Tissue Kit with the DNase-treatment step included (Cat. No. 12033674001, Roche). The RNA yield and purity were estimated using Nanodrop (Cat. No. 9380, ND-1000 UV/Vis, Nanodrop Spectrophotometer, USA) and Agilent 2100 Bioanalyzer (Cat. No. DE00001234, Agilent Technologies, CA, USA). For the skin necropsies (given their small size, ~3 × 2 mm patch), the RNA concentrations ranged between 1 and 10 ng/μl with RNA Integrity Number (RIN) > 6.0, A260/280 values between 1.6 and 2.11 and A260/230 values between 1.52 and 2.48 while for the brain samples (~8 mm^3) the RNA concentrations ranged between 8 and 160 ng/μl with RIN >9.5, A260/280 values between 2.01 and 2.24 and A260/230 values between 2.16 and 2.37.

The library preparation and sequencing were performed at the European Molecular Biology Laboratory (EMBL), Heidelberg, Germany. All the samples were first barcoded with Illumina TruSeq adapters. The NGS libraries were prepared using two different approaches, namely the RNA-seq and QuantSeq. The RNA-seq libraries were generated from the whole RNA and QuantSeq sequences were generated from the RNA 3′ends. The RNA-seq libraries were prepared using NEBNext Ultra II Directional RNA Library Prep Kit for Illumina, and the QuantSeq libraries were prepared using Lexogen QuantSeq 3′ polyadenylated RNA Library Prep Kit FWD for Illumina. For both applications, the sequencing was carried out using the Illumina NextSeq 500 platform, with the RNA-seq reads being 80 base pair (bp) paired-end (PE), and the QuantSeq reads being 80 bp single-end (SE).

For the RNA-seq we sequenced skin samples (left wing patagium) from six randomly selected treatment individuals, representing their LPS-stimulated wing-web skin (hereafter referred to as 'treatment-treatment', tt), the control skin samples (right wing patagium) from the same six LPS-stimulated individuals (hereafter referred to as 'control-treatment', ct) and unmanipulated skin samples (left wing patagium) from six randomly chosen control individuals (hereafter referred to as 'control-control', cc). The general immune response was estimated by comparing cc samples to tt samples. The comparison of ct samples to tt samples served us for description of the relative effects of the local immune response, while the comparison of cc samples to ct samples served us to disentangle the effects of the systemic immune responses in the periphery. To reach comparable sequencing costs for both approaches focusing on the tt and cc comparison, for QuantSeq we compared 12 treatment skin samples from the treatment individuals (tt) to 12 control skin samples from the control individuals (cc). Using the advantage of the cost-efficient QuantSeq approach, we were able to cover larger population sample and hence overcome the issue of inter-individual variability in transcriptomic patterns biasing the results. Finally, to meet our main objective, using QuantSeq we sequenced brain samples from the same 12 treatment individuals and 12 control individuals. The raw sequences were uploaded in the Sequence Read Archive (SRA) of NCBI (accession number: PRJNA751848).

2.3. Transcriptome bioinformatics

The transcriptome bioinformatic analysis was carried out in Wageningen University and Research (WUR), the Netherlands. The BAQCOM pipeline v. 0.3.2 (https://github.com/hanielcedraz/BAQCOM; Adapter trimming: Trimmomatic v. 0.39; Alignment STAR v. 2.7.2b; Readcounts: featurecounts v. 2.0.3) with the zebra finch reference genome (Taeniopygia_guttata.bTaeGut1_v1.p.dna.toplevel.fa) and annotation file (Taeniopygia_guttata.bTaeGut1_v1.p.108.gtf) downloaded from Ensembl (Howe et al., 2021) was adopted for the data analysis. This was based on initial testing of the BAQCOM and the bluebee pipeline (https://www.bluebee.com/lexogen/; Adapter trimming: bbduk v. 35.92; Alignment STAR v. 2.5.2a; Readcounts: HTSeq-count v. 0.6.0).

On average, the RNA-seq generated in the skin samples ~130 million reads per individual (range from 85,612,614 to 167,895,520 reads; Table S3, ESM1) with the alignment percentage ranging between 55.50% and 95.98% (Table S4, ESM1). For QuantSeq, the sequence data obtained were on average ~9.5 million reads per individual (range from 1,586,888 to 21,400,263 reads) for the skin samples and ~13.4 million reads per individual (range between 11,309,173 and 16,028,933 reads; Table S3, ESM1) for the brain samples. For the skin samples, the alignment percentage ranged between 65.56% and 95.86% and for the brain samples, the alignment percentage ranged between 68.99% and 91.38% (Table S4, ESM1).

As outlined above, for DEG analysis in RNA-seq data we used the in-depth capacity of the platform to gain insight into the additive effects of local and systemic immune response: i) the general response was estimated by comparing the groups cc vs. tt (as for the QuantSeq), ii) the local effects were estimated by comparing treatment and control wings

from the same treatment individuals (ct vs. tt), and finally iii) the systemic effects were estimated by comparing unmanipulated controls to untreated skin in the intraabdominally LPS-injected individuals (cc vs. ct). The DESeq2 program was used with default settings to calculate the fold change gene expression values that were then transformed to their $\log_2$ values. Genes with padj value ≤ 0.05 and a $\log_2$ fold change value ≥ 1 were considered as significantly differentially expressed. Gene functional annotations (gene ontology, GO) were attributed using the Ensembl BioMart (Smedley et al., 2015) with a zebra finch reference, manually supplemented with Uniprot (The UniProt Consortium et al., 2021) annotations. The GO terms for unannotated genes were assigned by finding orthologous genes in the chicken or human reference using gprofiler (Raudvere et al., 2019).

To reveal similarities and differences in the results obtained through the RNA-seq and QuantSeq platforms, we used the Co-Inertia multivariate Analysis (CIA) (Dolédec and Chessel, 1994; Dray et al., 2003) combined with the Monte Carlo permutation test (see Bílková et al., 2018). CIA identifies co-relationships between the samples from the same individuals represented in multiple datasets. Furthermore, the correlations between the QuantSeq and RNA-seq data were analysed using corrplot package (Version 0.84) and Spearman's correlation in R software (version 4.1.1; (Team, 2013). Since the total number of experimental animals differed between our RNA-seq and QuantSeq datasets, we applied these two approaches on identically subsampled datasets, using only the QuantSeq data from samples simultaneously sequenced also through the RNA-seq. We also ran the GATK (Genome Analysis Toolkit) pipeline (Poplin et al., 2017) to check for the relatedness-independent assortment of the individuals between the treatment groups; we used SNPRelate package (default settings) (Zheng et al., 2012) in R software for generating the dendrogram of individual relatedness. The result showed us that the birds were distributed between the treatment groups randomly with respect to their relatedness (Supplementary Fig. S1, ESM2). We generated Venn diagrams to indicate the DEGs common between the all the full length RNA-seq comparisons (RS) as well as between all RS vs. QuantSeq (QS) comparisons using Venny (version 2.1.0) (Oliveros, 2007). We used online tool ShinyGO v. 0.77 (http://bioinformatics.sdstate.edu/go/) to generate the gene interaction network for the differentially expressed genes from the QS data of both skin and brain tissues (Ge et al., 2020).

2.4. RT-qPCR validation of the gene expression changes in brain and skin

For the selected top DEGs (based on the fold change values from the QuantSeq analysis) expressed in both brain and skin we verified the expression patterns using RT-qPCR. The target genes included *IL1B*, avidin (*AVD-like*), antimicrobial protein avian β defensin 10 (*AvBD10*), two chemokine genes *CXCLi1, CXCLi2* (orthologous genes for the chemokine *CXCL8* ~ *IL8* in mammals; Poh et al., 2008) and anti-inflammatory gene aconitate decarboxylase 1 (*ACOD1*). The *28S rRNA* was used as a reference gene. The RT-qPCR was performed in triplicates, together with plate negative (no-template triplicate) and positive (standard dilution series 10^2-10^8 copies) controls, using Luna Universal Probe One-Step RT-PCR Kit (E3006, BioLabs Inc.) with 0.6 mM primer and 0.2 mM probe concentrations in a Light Cycler LC480 Instrument (Roche Diagnostics, Rotkreuz, Switzerland) set to cycling conditions: (1) 50 °C 10 min, (2) 95 °C 1 min, (3) (95 °C 10 s, 60 °C 30 s) × 45. The RNA for the RT-qPCR analysis was diluted in molecular water enriched with carrier-tRNA (Qiagen, Cat. No. 1068337): 1:5 for the target gene quantification and 1:500 for the reference gene (28S rRNA) quantification. Details to the RT-qPCR assays are provided in Table S5, ESM1. As positive controls we used the synthetic DNA standards (g-Blocks; Table S6, ESM1). Our assay efficiency was on average 1.911 (ranging between 1.72 and 2.00, Table S6, ESM1; standard curves for the RT-qPCR assays are provided in Fig. S2, ESM2). Prior the RT-qPCR analysis, we checked the sequence population variability in the primers and probes used for our RT-qPCR assays to identify any possible mismatches (extraction of genomic DNA from blood of 10 zebra finches using DNeasy Blood & Tissue Kit, Qiagen, cat. number 69581; amplification with Qiagen Multiplex PCR Plus kit in a reaction with 0.2 μM final concentration of primers; Sanger sequencing of the targets with BigDye Terminator v. 3.1 Cycle Sequencing Kit and 3500xL Genetic Analyzer Applied Biosystem platform). In the final assays that we designed for this study we did not find any sequence variation that could differentially affect the assay efficiencies between individuals (GenBank IDs are provided in Table S7, ESM1).

The gene expression quantification was calculated either as standard gene expression quantity (Qst; Vinkler et al., 2018) that allows comparison of the gene expression between treatments and controls or as the relative gene expression ratio (R) which provides the measure of gene expression fold change in the treatments against the controls (Pfaffl, 2001). In the *ACOD1* gene, non-specificities were repeatedly revealed when amplifying different regions of the gene with different combinations of primer pairs, probably resulting from repetitive GCs, indels variable in the population or multiple isoforms. Also, the efficiency of our *ACOD1* qPCR was very low in this gene (1.72). Therefore, *ACOD1* was excluded from the final DGE analysis. The analysis was limited only to the top target genes and a single reference gene because of the low amounts of RNA that was remining after the transcriptomics and was available for the RT-qPCR analysis.

The statistical analysis of the RT-qPCR results was conducted using the R software (Team, 2013). We assessed data normality distribution through the Shapiro-Wilk test. Due to the non-normal distribution of the Qst values, we opted to employ the non-parametric Wilcox test for further analysis. The differences in gene expression between treatment groups were visualised as boxplots using the *ggplot2* package (v. 3.4.2). Correlation tests and Principal Component Analyses (PCA) were performed for the selected genes studied via RT-qPCR in both skin and brain tissues, respectively. The relative expression data were normalized using a common logarithm.

3. Results

3.1. Skin swelling response to LPS stimulation

Before transcriptomic analysis, we checked whether the inflammatory immune response to the LPS stimulation occurred in skin of the treatment birds in the time of tissue collection. This was revealed by the significant swelling of the tissue in treatments compared to controls (Wilcoxon signed rank test: $n = 24$, $V = 1.00$, $p = 0.003$; Fig. 1).

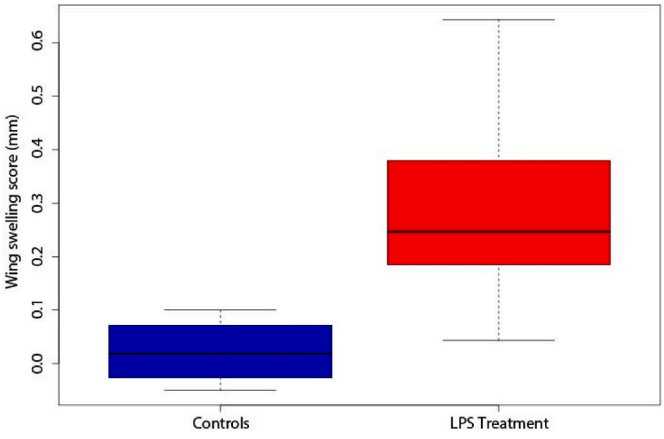

Fig. 1. Difference in the wing patagium swelling response between the LPS-treatment birds and controls. The wing swelling score was used as an inflammatory response measure, calculated as the difference in skin thickness between the left (treatment) wing patagium and the right (control) wing patagium (mm). Mean and variation in SD is shown.

3.2. Skin transcriptomics analysed by the RNA-seq approach

Based on the zebra finch RNA-seq data from skin peripheral inflammation, our experimental design allows us to elucidate the relative effects of systemic and local responses from the general transcriptomic changes. First, the DGE analysis of the general response (tt vs. cc; dataset RS1) revealed in total 370 DEGs with 117 of them having annotation of the gene function. Out of these 62 were up-regulated and 57 down-regulated (gene list with GO annotations provided in Table S8, ESM1). Interestingly, the most significant up-regulated genes belonged to the GO terms muscle fibre development pathway, positive regulation of Rho protein signal transduction pathway and post-translational protein modification pathway. Only six upregulated genes were involved in immune function, including innate immune response (*SUSD4*), leukocyte migration involved in inflammatory response (*TRIM55*) and negative regulation of interferon-gamma-mediated signalling pathway (*PPARG*). Neither most of the significantly down-regulated genes were involved in immune function; those that were (5 genes) belonged to the pathways including negative regulation of inflammatory response (*CCN3*) and positive regulation of interleukin-1 production (*PANX2*). Second, analysis of the local effects of the LPS treatment (ct vs. tt; dataset RS2) identified 103 DEGs out of which only 43 DEGs had gene function annotations, with as few as 14 up-regulated ones and the remaining 29 genes being down-regulated (Table S9, ESM1). The most significant up-regulated genes belonged to the regulation of apoptotic process and activation of JUN kinase activity pathways. Minority of the up-regulated DEGs were associated with immunity: inflammatory response (*KLRG1*), response to bacterium (*CLPS*) and cytokine-mediated signalling pathway (*IL17RD*). Key down-regulated genes belonged to the following pathways: intracellular signal transduction, lipid metabolic process, and calcium ion transport. Among the few down-regulated immune genes belonged those linked with negative regulation of NIK/NF-kappaB signalling (*CCN3*), positive regulation of interleukin-1 production (*PANX2*) and innate immune response (*POLR3E*). Third, analysis of the systemic effects of the peripheral LPS stimulation (cc vs. ct; dataset RS3) identified 76 DEGs in total, but only 37 genes annotated. Among these, 33 were up-regulated and 4 down-regulated (Table S10, ESM1). The main pathways identified were partially consistent with the results of our general (cc-tt; RS1) analysis, although we could only find a single gene which was directly involved in immune function (*ANKRD1*).

We found limited overlaps between the gene sets revealed by the three separate DGE analyses, with no genes common among all of them (Fig. S3; Table S11, ESM1). There were 32 genes common between RS1 and RS2, indicating their involvement in the local response, although only a single one (*BIRC7*) showed a direct immune function). There were 25 genes common between RS1 and RS3, suggesting their role in systemic response, but none had any specific role in immunity. Thus, surprisingly, our RNA-seq analysis did not reveal any important involvement of immune genes in the immune response. Therefore, we conclude that within the existing budget constraints, our RNA-seq was not very successful in detecting the immunological effect of an avian systemic inflammation. These pilot results indicated that simple increase in the sample size and sequencing depth would not be a cost-effective and budget-feasible solution to reach our objective. Therefore, an alternative strategy was adopted, applying the QuantSeq approach to identify the immunological effect of the LPS stimulations.

3.3. Skin transcriptomics analysed by the QuantSeq approach

In an enlarged dataset of 24 individuals potentially better representing the inter-individual variation, we analysed the general skin inflammatory response (cc vs. tt) using the QuantSeq approach (dataset QS; equivalent RS1). We identified the differential expression in 265 genes. Out of the 168 significant DEGs with functional annotation available, 113 genes were up-regulated, and 55 genes were down-regulated (Table S12, ESM1; the gene interaction networks for the up-regulated and down-regulated genes are shown in Fig. S4 and Fig. S5, respectively). In contrast to the RS1 dataset, several of the up-regulated DEGs represented key regulators of immune response and known inflammation markers. As expected, the major immune pathways detected were immune response (*SCAP*), innate immune response (*CXCL8*), and cellular response to lipopolysaccharide (*IL1B, TNIP3*). Our analysis also identified changes in expression of other genes functionally related with altered physiology during inflammation, including, e.g., cell-cell junction assembly (*CDH12*), maintenance of epithelial cell apical/basal polarity (*LHX2*) and anatomical structure morphogenesis (*SOX3*).

We found little overlap between the most significant up-regulated pathways revealed by the four skin sample comparisons we performed (Fig. 2). Searching for possible overlaps (Fig. 3), we found only 6 DEGs with defined GO annotation common between the RNA-seq and QuantSeq results (cc-tt) in skin: *MB*, *MYOZ1*, *CKMT2*, *MYL1*, *TNNT3* and *PLCXD3* with most of them having their roles in skeletal muscle development and muscle contraction, but no associations to immunity. Yet, CIA showed significant co-structure between the RNA-seq and QuantSeq datasets (RV = 0.445, Monte Carlo test p = 0.001), indicating that both approaches captured at least part of the same biologically relevant differences between the samples (Table S13, ESM1).

3.4. Identification of differentially expressed genes in brain during peripheral inflammation

We used the QuantSeq approach to identify also suitable neuroinflammatory markers in the zebra finch. Our analysis of DGE in the hyperpallial region of brain in the full dataset of 24 individuals identified seven consistently represented DEGs, out of which 6 genes were up regulated (Table S14, the gene interaction network is shown in Fig. S6). The up-regulated genes refer to pathways involved in antibacterial humoral response (*AVD-like*), cellular response to interleukin-1 (*ACOD1*), inflammatory response (*EX-FABP-like*), clustering of voltage-gated sodium channels (*GLDN*), iron ion transport (*FTH1*) and positive regulation of Notch signalling pathway (*BMP2K*; Fig. 4). The single down-regulated gene is *MIR29B2*, which is a miRNA with unknown function in birds. *AVD-like* and *ACOD1* were then selected as our putative neuroinflammatory markers. CIA showed significant co-structure between the brain and skin QuantSeq datasets (RV = 0.33, Monte Carlo test p = 0.001; Table S15).

3.5. Validation of the QuantSeq-identified DEGs in skin and brain using RT-qPCR

To verify the accuracy of the QuantSeq estimates of gene expression changes during inflammation in the zebra finch, 5 selected DEGs (*IL1B*, *AvBD10*, *AVD-like*, *CXCLi1* and *CXCLi2*) identified in either skin or brain were targeted by the RT-qPCR (details on the RT-qPCR results are provided in Table S16). Unfortunately, we were unable to develop a functional RT-qPCR for *ACOD1* where we experienced non-specificities in amplified products (Table S5 and Table S6 in ESM1). In skin, we found that expression of all the 5 remaining genes was significantly up-regulated, consistently with our QuantSeq results (Table S12). Interestingly, this trend was not captured by the RNA-seq, which showed no significant difference in the expression of these genes in skin (Fig. 5). The expression of several of these selected genes in skin, as revealed by the RT-qPCR, was intercorrelated, but did not correlate with the metrical measurement of the skin swelling (Table S17). Also the PCA analysis of the RT-qPCR gene expression data in skin showed that all the tested genes consistently followed the same trend of activation (PC1 explained 61.8% of the variation, PC2 explained 20.9% of the variation; Fig. S7). In the brain, the PCA showed two gene clusters, one formed by *AvBD10* and *CXCLi1* and the other one by *IL1B*, *AVD-LIKE* and *CXCLi2* (PC1 explained 66.9% variability, PC2 explained 18.5% of the variation; Fig. S7). The correlation matrices for *IL1B*, *AVD-LIKE*, *AvBD10*, *CXCLi1*

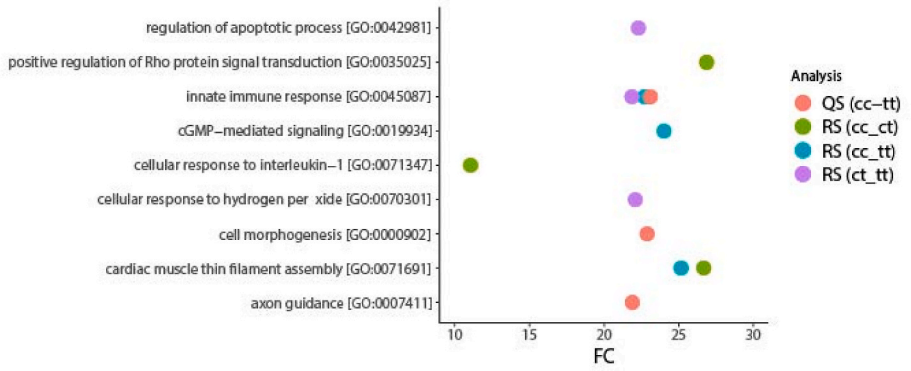

Fig. 2. The most significant up-regulated pathways revealed in the four transcriptomic analyses of the skin peripheral response to bacterial lipopolysaccharide (LPS) in the zebra finch. Two approaches (RS = RNA-seq and QS = QuantSeq) were adopted to reveal the differential gene expression between skin samples obtained from control patagium tissue in control individuals (cc), control patagium tissue in treatment individuals (ct) and treatment patagium tissue in treatment individuals (tt), x-axis shows $\log_2$ fold change (FC), y-axis shows the most significant pathways.

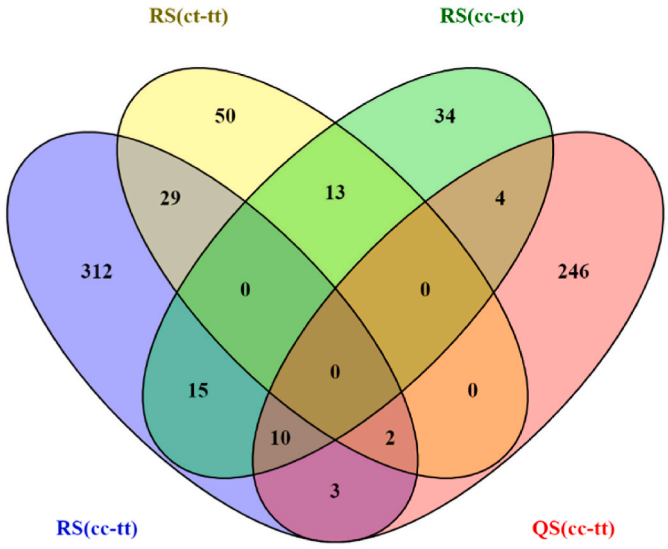

Fig. 3. Venn diagram showing the number of common differentially expressed genes between the four transcriptomic analyses of the skin peripheral response to bacterial lipopolysaccharide (LPS) in zebra finch. Two approaches (RS = RNA-seq and QS = QuantSeq) were adopted to reveal the differential gene expression between skin samples obtained from control patagium tissue in control individuals (cc), control patagium tissue in treatment individuals (ct) and treatment patagium tissue in treatment individuals (tt).

and *CXCLi2* showing the RT-qPCR-detected gene expression trends for brain and skin are provided in the supplementary files (Table S18 and Table S19 in ESM1, and Fig. S8 and Fig. S9 in ESM2). None of the cytokine genes serving as peripheral inflammatory markers (*IL1B*, *CXCLi1* and *CXCLi2*) was in the brain differentially expressed between the treatments and the controls (in all cases $p > 0.100$). This result was again consistent with the QuantSeq results. In contrast, *AVD-like* gene expression up-regulation was detected by RT-qPCR in the brain, validating the QuantSeq results (Fig. 5; rest of the figures are provided in Fig. S10 and Fig. S11 in ESM2). Furthermore, we found increased expression of *AvBD10* gene in the brain of the LPS-stimulated individuals, which was not captured by the QuantSeq transcriptomics. For all the selected genes in skin (*AVD-like*: $r = 0.751$, $p \ll 0.001$; *AvBD10*: $r = 0.758$, $p \ll 0.001$; *CXCLi1*: $r = 0.797$, $p \ll 0.001$; *CXCLi2*: $r = 0.621$, $p = 0.001$; *IL1B*: $r = 0.489$, $p = 0.015$) and for *AVD-like* in brain ($r = 0.581$, $p < 0.003$) we found strong correlations between the QuantSeq and RT-qPCR data (for *AVD-like* shown in Fig. 5, for the other four genes expressed in skin and brain see Figs. S12 and S13 in ESM2). Our results indicate that within comparable expense limits, the QuantSeq method showed improved sensitivity over to the traditional RNA-seq to the changes in expression of the immune genes.

4. Discussion

Diverse transcriptomic methods are now available to analyse variation in gene expression, but not all are equally suitable for all types of datasets. Our initial attempts to describe the gene expression patterns during local and systemic immune response to LPS using RNA-seq in 12

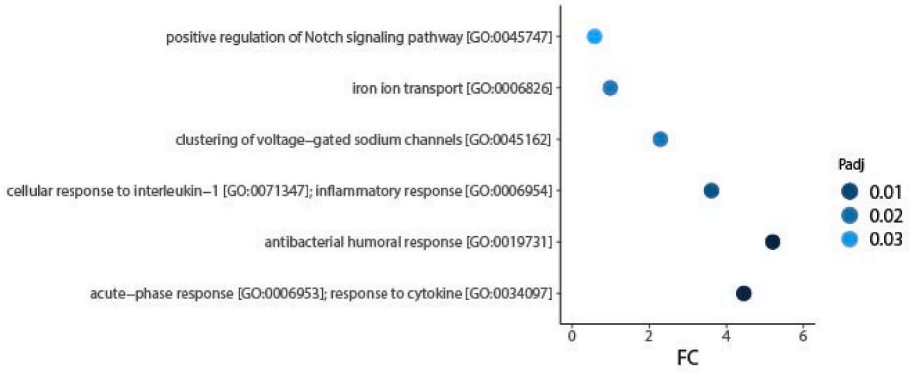

Fig. 4. The most significant up-regulated pathways revealed in the transcriptomic analysis of the brain response to peripheral stimulation with bacterial lipopolysaccharide (LPS) in zebra finch. QuantSeq (QS) approach was adopted to reveal differential gene expression, x-axis shows $\log_2$ fold change (FC), y-axis shows the most significant pathways.

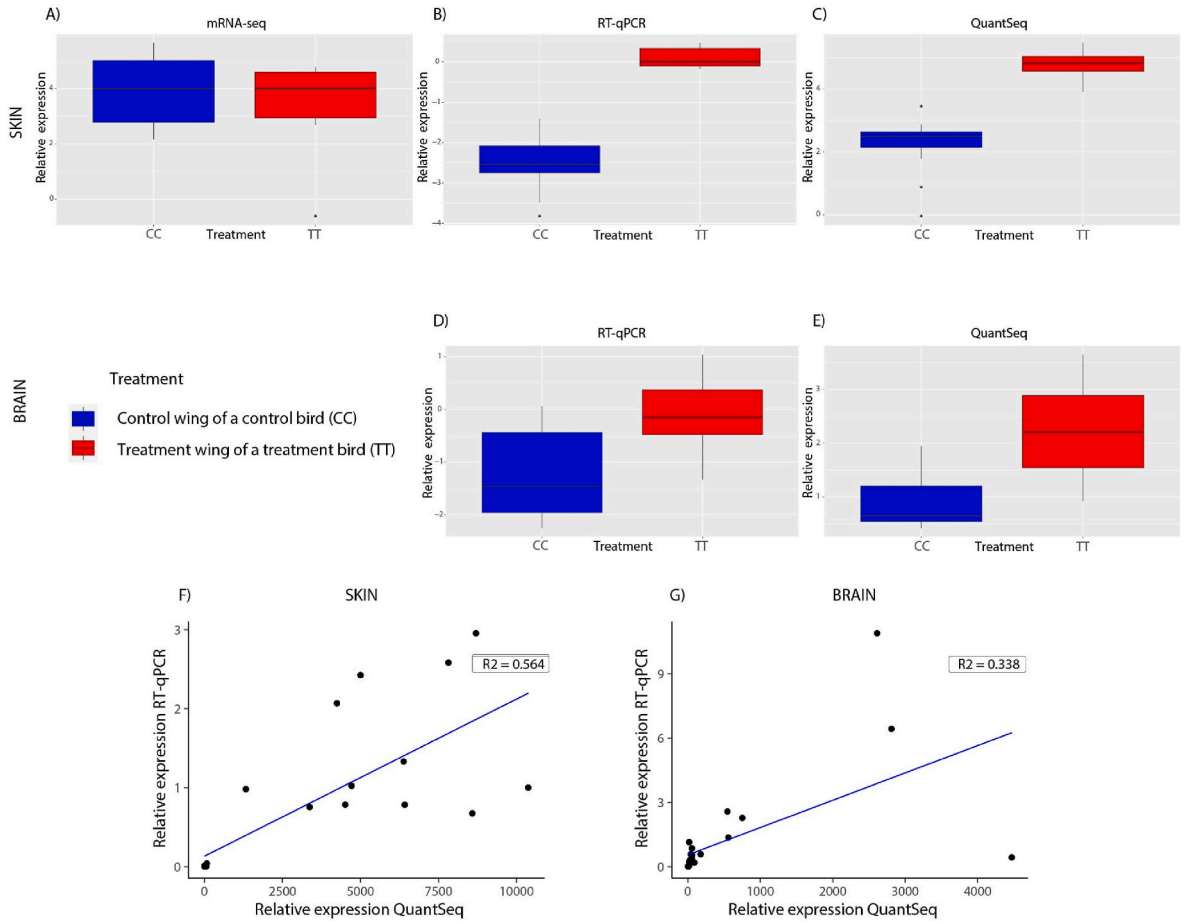

Fig. 5. Expression changes in the *AVD-like* gene estimated through (A) RNA-seq (RS1), (B) RT-qPCR, (C) QuantSeq approaches in the skin samples of controls (CC) and treatment individuals (TT) with peripheral response stimulated with bacterial lipopolysaccharide (LPS) in zebra finch. (D) RT-qPCR and (E) QuantSeq show *AVD-like* gene expression in brain during this peripheral response. Correlation between the RT-qPCR and QuantSeq data on the *AVD-like* gene expression in skin, $r = 0.751$, $p << 0.001$ (F) and in brain, $r = 0.581$, $p = 0.003$ (G).

zebra finch individuals (6 control and 6 treatment birds) revealed much inconsistency to Scalf et al. (2019) regarding the immune gene expression. Assuming that high inter-individual variation in our experimental zebra finch dataset could have contributed to this result, we opted another library preparation technique, the QuantSeq. Using the single 3′end sequencing, the cost efficiency of this approach (per sample 1/5th of the RNA-seq price) allowed us to increase the sequenced transcriptomic dataset, consisting of skin and brain samples, to 24 individuals (12 control and 12 treatment birds). Based on this approach we were able to identify candidate genes expressed in brain during peripheral inflammation. Our RT-qPCR analysis in selected genes validated the application of the QuantSeq method for identification of immune gene expression changes in the genetically heterogeneous domestic zebra finch model.

Given the dynamics of the immune response, timing of the response measurement is an important parameter in characterisation of inflammation. In our study we selected the 24-h response period, because this timing is often adopted in studies aimed at investigation of the skin immune responsiveness in passerine birds, corresponding to the peak of the tissue swelling response (Vinkler et al., 2010). Our result evidence significant tissue swelling at 24 h after stimulation, which is assumed to reflect tissue infiltration with various leukocyte types (Martin et al., 2006). Based on the understood molecular mechanism of the immune stimulation with LPS in the zebra finch (Vinkler et al., 2009), our experiment characterises gene expression changes during non-specific sterile inflammation activated in the skin through TLR4-mediated signalling.

Consistent with results of other studies (Jarvis et al., 2020; Vo et al., 2021), we show important differences between the DGE analysis results obtained through the RNA-seq and the QuantSeq approaches. While in the skin response the RNA-seq method identified more DEGs in total (371 genes compared to 265 genes identified by the QuantSeq method), this difference did not hold for the subset of the genes with available databased annotations, where QuantSeq provided more results (168 genes compared to only 120 genes detected by the RNA-seq approach). The two approaches differ in the depth of sequencing, with the QuantSeq having higher coverage, but only in a much shorter part of the full-length transcript than RNA-seq. We assume that most of the unannotated genes could be sequences of non-coding RNAs in which the function is typically not known in less frequently studied species. Thus, for the zebra finch population datasets, the QuantSeq approach appears as a more cost-effective approach to identify the gene expression changes associated with inflammatory response. Similar to our findings, previous research reported that RNA-seq identifies in general more DEGs, but QuantSeq can detect more transcripts with specific features, e.g. shorter genes (Ma et al., 2019) that often act in immunity as effector and signalling molecules (Vo et al., 2021). It is important to note that although we sequenced lower number of samples using the RNA-seq method than using QuantSeq, the number of samples analysed by RNA-seq was still comparable to many other transcriptomic experiments in model organisms, e.g. in laboratory rodents (Liu et al., 2021; Söllner et al., 2017). However, the domestic zebra finch population is genetically more heterogenous than the common laboratory models (Forstmeier et al., 2007; Gasch et al., 2016), which can affect the levels of

inter-individual variation in immune responsiveness and decrease power of the DGE analysis. Yet, the results of our CIA indicate that despite this issue, both the RNA-seq and QuantSeq approaches captured in the zebra finch biologically relevant variation between the samples analysed, documenting the relevance of those results that we were able to obtained. Comparisons of the local (ct vs. tt) and systemic response (cc vs. ct) using the RNA-seq generally showed pathways unrelated to immunity. Interestingly, in skin there were just 15 DEGs in common between the RNA-seq and QuantSeq results, out of which six genes only had defined gene names and functions. All the six shared genes were down-regulated in both RS1(cc-tt) and QS(cc-tt) and were mainly involved in movement physiology, suggesting changes in the physiology of subcutaneous muscles towards movement restrictions during the sickness phase, commonly observed during later stages of the acute response (Adelman et al., 2013; Deak et al., 2005; Sköld-Chiriac et al., 2014). Similar results were described earlier in fish and mammals (Brant et al., 2019; Liu et al., 2022; Sousa et al., 2022).

Importantly, the QuantSeq approach identified 56 genes involved in immune function whereas the RNA-seq only identified 12 immune genes as DEGs. Using the QuantSeq approach, we revealed in the skin up-regulation of key inflammation markers such as *IL1B* (Bent et al., 2018; Kaneko et al., 2019) and *CXCL8(IL8)* (Bent et al., 2018; Bernhard et al., 2021; Lopez-Castejon and Brough, 2011; Shahzad et al., 2010), showing the ongoing acute inflammation in the periphery (Lopez-Castejon and Brough, 2011). Our RT-qPCR results obtained from skin samples validate the QuantSeq results, but contradict the negative results obtained from RNA-seq (all the five genes tested).

Studies in rodents have shown that IL1B expressed in the periphery can activate both astrocytes and microglia in the brain, triggering neuroinflammation (Shaftel et al., 2008). *IL8* has a role in neutrophil activation and chemotaxis within the CNS during inflammation. In human microglia *IL8* levels increase in response to LPS (Ehrlich et al., 1998). *IL1B* also promotes the expression of avian β-defensins, which are important antimicrobial peptides (Hancock and Diamond, 2000; McDermott, 2004; Scott and Hancock, 2000). Especially *AvBD10* has been reported in the brain tissues of many avian species (Li et al., 2015). Our RT-qPCR captured similar *AvBD10* gene expression change in the brain that remained unidentified through the transcriptomics.

Unlike previous research of zebra finch neuroinflammation performed during the early phase of activation (2 h; Scalf et al., 2019), our study focused at the response observed 24 h after the LPS injection, identifying the delayed changes in gene expression. This could be responsible for the difference in the DGE pattern observed. In brain, our QuantSeq analysis identified only seven DEGs, i.e. less DEGs than identified during the early response (Scalf et al., 2019). Such a time-dependent change in the gene expression pattern is known also from mammalian studies (Rankine et al., 2006; Terenina et al., 2017). Yet, among the up-regulated DEGs detected in the brain, all six, *AVD-LIKE, EX-FABP-like, ACOD1, GLDN, FTH1, BMP2K*, are involved in immune response modulation, suggesting that expression of these genes could contribute to the regulation of neuroinflammation and related sickness physiology. Up-regulation of Avidin (*AVD*)-related genes is observed during inflammation and infections in chickens (Korpela et al., 1982; Kunnas et al., 1993). *AVD* up-regulation can induce expression of a stress protein family of Fatty acid-binding proteins (*FABPs*) (Zerega et al., 2001), lipid chaperones having a roles also in neurodegenerative diseases (Guo et al., 2022) and regulation of neuroinflammation (So et al., 2022, p. 4). Similar to our results, in chickens *EX-FABP* expression increases after stimulation with LPS and *IL6* (Cermelli et al., 2000), supporting the role of this gene in immunomodulation. Aconitate decarboxylase 1 (*ACOD1*, also known as immune responsive gene 1, *IRG1*) is a key regulator of immunometabolism during infection with important anti-inflammatory effects (Wu et al., 2022). In mice, both viral (Mills et al., 2018) and bacterial (Ganta et al., 2017; Shi et al., 2005) pathogens importantly enhance the expression of *ACOD1,* especially in microglia (Kanthasamy and Rangaraju, 2020). *FTH1* is known to be involved in macrophage activation, as evidenced by stimulation with LPS (Mesquita et al., 2020). Transcriptomics in mice microglial cells showed up-regulation of *FTH1* expression in late neurodegenerative diseases (Hunter et al., 2021). The associations of the remaining two DGEs with immunity are less direct, but previous studies showed elevated expression of bone morphogenetic protein 2 inducible kinase (*BMP2K*) during prolonged inflammation (Vance, 2014) and gliomedin (*GLDN*) is associated with profound macrophage infiltration into wounds and may be involved in the healing process (Etich et al., 2019).

To conclude, our results provide evidence for transcriptomic changes induced in the periphery (skin) by a local and systemic stimulation of inflammation, affecting gene expression regulation in the brain. These results on the late response complete the previously published evidence on early phases of the neuroimmune response to peripheral inflammation in the songbird model (Scalf et al., 2019). Twenty-four hours after stimulation the pro-inflammatory regulation is detectable in the periphery but has only very modest effects on the gene expression in zebra finch brain. Here the signalling is mostly anti-inflammatory, including up-regulated expression of genes involved in resolving the acute neuroinflammation. Further studies are required to bring understanding to the precise timing of the shift between neuroinflammatory and anti-inflammatory regulation and specific roles of individual genes and related pathways in this process, similar to the time scale experiments in rodent (Borniger et al., 2017; Lesur et al., 2010; Seok et al., 2013). Comparative research is key to reveal the basic principles of the neuro-immune interplay regulation. Our study including also the RT-qPCR validation indicates that specific cost-effective alternatives to the classical RNA-seq, such as the QuantSeq, can promote this demanding investigation in non-model, genetically heterogenous species, facilitating identification of key markers of peripheral inflammation and neuroinflammation applicable across species.

Statements and Declarations

The authors declare no potential conflicts of interest.

Author contributions

Conceptualization Ideas: Michal Vinkler, Nithya Kuttiyarthu Veetil.

Data curation: Nithya Kuttiyarthu Veetil.

Formal analysis: Nithya Kuttiyarthu Veetil, Mercedes Gomez-Samblas, Daniel Divín, Balraj Melepat.

Funding acquisition: Michal Vinkler, Nithya Kuttiyarthu Veetil, Balraj Melepat.

Investigation: Michal Vinkler, Nithya Kuttiyarthu Veetil, Daniel Divín, Eleni Voukali, Zuzana Świderska, Tereza Krajzingrová, Martin Těšický, Ferris Jung.

Methodology: Vladimír Beneš, Ole Madsen, Haniel Cedraz de Oliveira, Michal Vinkler, Nithya Kuttiyarthu Veetil.

Project administration: Michal Vinkler.

Software: Ole Madsen, Haniel Cedraz de Oliveira, Nithya Kuttiyarthu Veetil, Mercedes Gomez-Samblas.

Supervision: Michal Vinkler, Vladimír Beneš, Ole Madsen, Haniel Cedraz de Oliveira.

Visualization: Michal Vinkler, Nithya Kuttiyarthu Veetil, Mercedes Gomez-Samblas.

Writing – original draft: Nithya Kuttiyarthu Veetil, Michal Vinkler.

Writing – review & editing Preparation: Nithya Kuttiyarthu Veetil, Michal Vinkler, Mercedes Gomez-Samblas, Balraj Melepat, Ole Madsen, Haniel Cedraz de Oliveira, Vladimír Beneš, Ferris Jung, Daniel Divín, Eleni Voukali, Zuzana Świderska, Tereza Krajzingrová, Martin Těšický.

Data availability

Data will be made available on request.

Acknowledgements

This study was supported by Grant Schemes at Charles University (grant nos. GAUK 646119, PRIMUS/17/SCI/12, and START/SCI/113 with reg. no. CZ.02.2.69/0.0/0.0/19_073/0016935) and the Czech Science Foundation Grant No. P502/19-20152Y. The research visit of NKV to Wageningen University was supported by the Short-Term Scientific Mission programme of the European Cooperation in Science and Technology (COST) Action CA15112 (FAANG-Europe) and INTER-COST grant No. LTC18060 provided by the Ministry of Education, Youth and Sports of the Czech Republic. Computational resources were provided by the Wageningen University and data storage facility by the Czech Education and Scientific NETwork CESNET; project e-INFRA CZ LM2018140 supported by the Ministry of Education, Youth and Sports of the Czech Republic). We are also grateful to Martin Kocourek and Pavel Němec for the guidance in bird brain dissection. The study was further supported by the Institutional Research Support No. 260684/2023.

Appendix A. Supplementary data

Supplementary data to this article can be found online at https://doi.org/10.1016/j.dci.2023.105106.

References

Aamodt, C.M., Farias-Virgens, M., White, S.A., 2020. Birdsong as a window into language origins and evolutionary neuroscience. Philos. Trans. R. Soc. B. 375, 20190060. http://doi.org/10.1098/rstb.2019.0060.

Abou Elazab, M.F., Nasr, N.E., Ahmed, M.S., Alrashdi, B.M., Dahran, N., Alblihed, M.A., Elmahallawy, E.K., 2022. The effects of bacterial lipopolysaccharide (LPS) on Turkey poults: assessment of biochemical parameters and histopathological changes. Vet. Sci. 9, 240.

Adelman, J.S., Kirkpatrick, L., Grodio, J.L., Hawley, D.M., 2013. House finch populations differ in early inflammatory signaling and pathogen tolerance at the peak of *Mycoplasma gallisepticum* infection. Am. Nat. 181, 674–689. https://doi.org/10.1086/670024.

Arck, P.C., Slominski, A., Theoharides, T.C., Peters, E.M., Paus, R., 2006. Neuroimmunology of stress: skin takes center stage. J. Invest. Dermatol. 126, 1697–1704.

Arnaiz-Villena, A., Ruiz-del-Valle, V., Reche, P., Gomez-Prieto, P., Lowry, E., Zamora, J., Areces, C., Rey, D., Parga, C., Serrano-Vela, J.I., 2010. Songbirds conserved sites and intron size of MHC class I molecules reveal a unique evolution in vertebrates. Open Ornithol. J. 3, 156–165. https://doi.org/10.2174/1874453201003010156.

Asfor, A.S., Nazki, S., Reddy, V.R.A.P., Campbell, E., Dulwich, K.L., Giotis, E.S., Skinner, M.A., Broadbent, A.J., 2021. Transcriptomic analysis of inbred chicken lines reveals infectious bursal disease severity is associated with greater bursal inflammation in vivo and more rapid induction of pro-inflammatory responses in primary bursal cells stimulated ex vivo. Viruses 13, 933. https://doi.org/10.3390/v13050933.

Balakrishnan, C.N., Edwards, S.V., Clayton, D.F., 2010. The Zebra Finch genome and avian genomics in the wild. Emu - Austral Ornithol. 110, 233–241. https://doi.org/10.1071/MU09087.

Batra, T., Malik, I., Prabhat, A., Bhardwaj, S.K., Kumar, V., 2020. Sleep in unnatural times: illuminated night negatively affects sleep and associated hypothalamic gene expressions in diurnal zebra finches. Proc. R. Soc. A B 287, 20192952.

Becher, B., Spath, S., Goverman, J., 2017. Cytokine networks in neuroinflammation. Nat. Rev. Immunol. 17, 49–59. https://doi.org/10.1038/nri.2016.123.

Bent, R., Moll, L., Grabbe, S., Bros, M., 2018. Interleukin-1 beta—a friend or foe in malignancies? Int. J. Mol. Sci. 19, 2155.

Bernhard, S., Hug, S., Stratmann, A.E.P., Erber, M., Vidoni, L., Knapp, C.L., Thomaß, B.D., Fauler, M., Nilsson, B., Ekdahl, K.N., 2021. Interleukin 8 elicits rapid physiological changes in neutrophils that are altered by inflammatory conditions. J. Innate Immun. 13, 225–241.

Bílková, B., Świderská, Z., Zita, L., Laloë, D., Charles, M., Beneš, V., Stopka, P., Vinkler, M., 2018. Domestic fowl breed variation in egg white protein expression: application of proteomics and transcriptomics. J. Agric. Food Chem. 66, 11854–11863. https://doi.org/10.1021/acs.jafc.8b03099.

Bluthé, R., Bret-Dibat, J., Layé, S., Walter, V., Parnet, P., Lestage, J., Verrier, D., Poole, S., Stenning, B., Kelley, K., 1994. Cytokines induce sickness behaviour by a vagal mediated mechanism. J. Neuroimmunol. 54, 160.

Borniger, J.C., Walker II, W.H., Gaudier-Diaz, M.M., Stegman, C.J., Zhang, N., Hollyfield, J.L., Nelson, R.J., DeVries, A.C., 2017. Time-of-day dictates transcriptional inflammatory responses to cytotoxic chemotherapy. Sci. Rep. 7, 1–11.

Bramley, J.C., Collins, S.V.A., Clark, K.B., Buchser, W.J., 2016. Avian axons undergo Wallerian degeneration after injury and stress. J. Comp. Physiol. 202, 813–822. https://doi.org/10.1007/s00359-016-1123-y.

Brant, J.O., Boatwright, J.L., Davenport, R., Sandoval, A.G.W., Maden, M., Barbazuk, W. B., 2019. Comparative transcriptomic analysis of dermal wound healing reveals de novo skeletal muscle regeneration in Acomys cahirinus. PLoS One 14, e0216228.

Brites, D., Fernandes, A., 2015. Neuroinflammation and depression: microglia activation, extracellular microvesicles and microRNA dysregulation. Front. Cell. Neurosci. 9 https://doi.org/10.3389/fncel.2015.00476.

Canchi, S., Swinton, M.K., Rissman, R.A., Fields, J.A., 2020. Transcriptomic analysis of brain tissues identifies a role for CCAAT enhancer binding protein β in HIV-associated neurocognitive disorder. J. Neuroinflammation 17, 112. https://doi.org/10.1186/s12974-020-01781-w.

Casebere, K.R., Kaiser, M.G., Lamont, S.J., 2015. Bacterial component induced inflammatory response in roosters from diverse genetic lines. Iowa State Univ. Anim. Ind. Rep. 12.

Cermelli, S., Zerega, B., Carlevaro, M., Gentili, C., Thorp, B., Farquharson, C., Cancedda, R., Descalzi Cancedda, F., 2000. Extracellular fatty acid binding protein (Ex-FABP) modulation by inflammatory agents: "physiological" acute phase response in endochondral bone formation. Eur. J. Cell Biol. 79, 155–164. https://doi.org/10.1078/S0171-9335(04)70018-7.

Chen, Y., Lyga, J., 2014. Brain-skin connection: stress, inflammation and skin aging. Inflamm. Allergy-Drug Targets Former. Curr. Drug Targets-Inflamm. AllergyDiscontinued 13, 177–190.

Corley, S.M., Troy, N.M., Bosco, A., Wilkins, M.R., 2019. QuantSeq. 3′ Sequencing combined with Salmon provides a fast, reliable approach for high throughput RNA expression analysis. Sci. Rep. 9, 18895 https://doi.org/10.1038/s41598-019-55434-x.

Crowell, H.L., Soneson, C., Germain, P.-L., Calini, D., Collin, L., Raposo, C., Malhotra, D., Robinson, M.D., 2020. Muscat detects subpopulation-specific state transitions from multi-sample multi-condition single-cell transcriptomics data. Nat. Commun. 11, 6077. https://doi.org/10.1038/s41467-020-19894-4.

Danielski, L.G., Giustina, A.D., Badawy, M., Barichello, T., Quevedo, J., Dal-Pizzol, F., Petronilho, F., 2018. Brain barrier breakdown as a cause and consequence of neuroinflammation in sepsis. Mol. Neurobiol. 55, 1045–1053. https://doi.org/10.1007/s12035-016-0356-7.

David, M., Cézilly, F., Giraldeau, L.-A., 2011. Personality affects zebra finch feeding success in a producer–scrounger game. Anim. Behav. 82, 61–67. https://doi.org/10.1016/j.anbehav.2011.03.025.

Deak, T., Bellamy, C., Bordner, K.A., 2005. Protracted Increases in Core Body Temperature and Interleukin-1 Following Acute Administration of Lipopolysaccharide: Implications for the Stress Response 12.

DiSabato, D.J., Quan, N., Godbout, J.P., 2016. Neuroinflammation: the devil is in the details. J. Neurochem. 139, 136–153. https://doi.org/10.1111/jnc.13607.

Divín, D., Goméz Samblas, M., Kuttiyarthu Veetil, N., Voukali, E., Świderská, Z., Krajzingrová, T., Těšický, M., Beneš, V., Elleder, D., Bartoš, O., Vinkler, M., 2022. Cannabinoid receptor 2 evolutionary gene loss makes parrots more susceptible to neuroinflammation. Proc. R. Soc. B Biol. Sci. 289, 20221941 https://doi.org/10.1098/rspb.2022.1941.

Dolédec, S., Chessel, D., 1994. Co-inertia analysis: an alternative method for studying species–environment relationships. Freshw. Biol. 31, 277–294.

Dray, S., Chessel, D., Thioulouse, J., 2003. CO-INERTIA analysis and the linking of ECOlogical data tables. Ecology 84, 3078–3089. https://doi.org/10.1890/03-0178.

Du, Y., Li, X.-S., Chen, L., Chen, G.-Y., Cheng, Y., 2020. A network analysis of epigenetic and transcriptional regulation in a neurodevelopmental rat model of schizophrenia with implications for translational research. Schizophr. Bull. 46, 612–622. https://doi.org/10.1093/schbul/sbz114.

Ehrlich, L.C., Hu, S., Sheng, W.S., Sutton, R.L., Rockswold, G.L., Peterson, P.K., Chao, C. C., 1998. Cytokine regulation of human microglial cell IL-8 production. J. Immunol. 160, 1944–1948.

Ekblom, R., Balakrishnan, C.N., Burke, T., Slate, J., 2010. Digital gene expression analysis of the zebra finch genome. BMC Genom. 11, 1–13.

Erickson, M.A., Dohi, K., Banks, W.A., 2012. Neuroinflammation: a common pathway in CNS diseases as mediated at the blood-brain barrier. Neuroimmunomodulation 19, 121–130. https://doi.org/10.1159/000330247.

Eskew, E.A., Fraser, D., Vonhof, M.J., Pinsky, M.L., Maslo, B., 2021. Host gene expression in wildlife disease: making sense of species-level responses. Mol. Ecol. 30, 6517–6530. https://doi.org/10.1111/mec.16172.

Etich, J., Koch, M., Wagener, R., Zaucke, F., Fabri, M., Brachvogel, B., 2019. Gene expression profiling of the extracellular matrix signature in macrophages of different activation status: relevance for skin wound healing. Int. J. Mol. Sci. 20, 5086. https://doi.org/10.3390/ijms20205086.

Finotello, F., Di Camillo, B., 2015. Measuring differential gene expression with RNA-seq: challenges and strategies for data analysis. Brief. Funct. Genomics 14, 130–142. https://doi.org/10.1093/bfgp/elu035.

Flores-Santin, J., Burggren, W.W., 2021. Beyond the chicken: alternative avian models for developmental physiological research. Front. Physiol. 12, 712633 https://doi.org/10.3389/fphys.2021.712633.

Forstmeier, W., Segelbacher, G., Mueller, J.C., Kempenaers, B., 2007. Genetic variation and differentiation in captive and wild zebra finches (*Taeniopygia guttata*): zebra FINCH population genetics. Mol. Ecol. 16, 4039–4050. https://doi.org/10.1111/j.1365-294X.2007.03444.x.

Friedrich, S.R., Nevue, A.A., Andrade, A.L., Velho, T.A., Mello, C.V., 2022. Emergence of sex-specific transcriptomes in a sexually dimorphic brain nucleus. Cell Rep. 40.

Ganta, V.C., Choi, M.H., Kutateladze, A., Fox, T.E., Farber, C.R., Annex, B.H., 2017. A MicroRNA93–interferon regulatory factor-9–immunoresponsive gene-1–itaconic acid pathway modulates M2-like macrophage polarization to revascularize ischemic muscle. Circulation 135, 2403–2425. https://doi.org/10.1161/CIRCULATIONAHA.116.025490.

Gasch, A.P., Payseur, B.A., Pool, J.E., 2016. The power of natural variation for model organism Biology. Trends Genet. 32, 147–154. https://doi.org/10.1016/j.tig.2015.12.003.
Ge, S.X., Jung, D., Yao, R., 2020. ShinyGO: a graphical gene-set enrichment tool for animals and plants. Bioinformatics 36, 2628–2629.
Guo, Q., Kawahata, I., Cheng, A., Jia, W., Wang, H., Fukunaga, K., 2022. Fatty acid-binding proteins: their roles in ischemic stroke and potential as drug targets. Int. J. Mol. Sci. 23, 9648. https://doi.org/10.3390/ijms23179648.
Hancock, R.E.W., Diamond, G., 2000. The role of cationic antimicrobial peptides in innate host defences. Trends Microbiol. 8, 402–410. https://doi.org/10.1016/S0966-842X(00)01823-0.
He, J., Fu, T., Zhang, L., Gao, L.W., Rensel, M., Remage-Healey, L., White, S.A., Gedman, G., Whitelegge, J., Xiao, X., 2022. Improved zebra finch brain transcriptome identifies novel proteins with sex differences. Gene 843, 146803.
Hellgren, O., Ekblom, R., 2010. Evolution of a cluster of innate immune genes (β-defensins) along the ancestral lines of chicken and zebra finch. Immunome Res. 6, 3. https://doi.org/10.1186/1745-7580-6-3.
Hernández-Romero, M.C., Delgado-Cortés, M.J., Sarmiento, M., de Pablos, R.M., Espinosa-Oliva, A.M., Argüelles, S., Bández, M.J., Villarán, R.F., Mauriño, R., Santiago, M., Venero, J.L., Herrera, A.J., Cano, J., Machado, A., 2012. Peripheral inflammation increases the deleterious effect of CNS inflammation on the nigrostriatal dopaminergic system. Neurotoxicology 33, 347–360. https://doi.org/10.1016/j.neuro.2012.01.018.
Hong, M., Tao, S., Zhang, L., Diao, L.-T., Huang, X., Huang, S., Xie, S.-J., Xiao, Z.-D., Zhang, H., 2020. RNA sequencing: new technologies and applications in cancer research. J. Hematol. Oncol.J Hematol Oncol 13, 1–16.
Howe, K.L., Achuthan, P., Allen, James, Allen, Jamie, Alvarez-Jarreta, J., Amode, M.R., Armean, I.M., Azov, A.G., Bennett, R., Bhai, J., Billis, K., Boddu, S., Charkhchi, M., Cummins, C., Da Rin Fioretto, L., Davidson, C., Dodiya, K., El Houdaigui, B., Fatima, R., Gall, A., Garcia Giron, C., Grego, T., Guijarro-Clarke, C., Haggerty, L., Hemrom, A., Hourlier, T., Izuogu, O.G., Juettemann, T., Kaikala, V., Kay, M., Lavidas, I., Le, T., Lemos, D., Gonzalez Martinez, J., Marugán, J.C., Maurel, T., McMahon, A.C., Mohanan, S., Moore, B., Muffato, M., Oheh, D.N., Paraschas, D., Parker, A., Parton, A., Prosovetskaia, I., Sakthivel, M.P., Salam, A.I.A., Schmitt, B.M., Schuilenburg, H., Sheppard, D., Steed, E., Szpak, M., Szuba, M., Taylor, K., Thormann, A., Threadgold, G., Walts, B., Winterbottom, A., Chakiachvili, M., Chaubal, A., De Silva, N., Flint, B., Frankish, A., Hunt, S.E., Iisley, G.R., Langridge, N., Loveland, J.E., Martin, F.J., Mudge, J.M., Morales, J., Perry, E., Ruffier, M., Tate, J., Thybert, D., Trevanion, S.J., Cunningham, F., Yates, A.D., Zerbino, D.R., Flicek, P., 2021. Ensembl 2021. Nucleic Acids Res. 49, D884–D891. https://doi.org/10.1093/nar/gkaa942.
Hunter, M., Spiller, K.J., Dominique, M.A., Xu, H., Hunter, F.W., Fang, T.C., Canter, R.G., Roberts, C.J., Ransohoff, R.M., Trojanowski, J.Q., Lee, V.M.-Y., 2021. Microglial transcriptome analysis in the rNLS8 mouse model of TDP-43 proteinopathy reveals discrete expression profiles associated with neurodegenerative progression and recovery. Acta Neuropathol. Commun. 9, 140. https://doi.org/10.1186/s40478-021-01239-x.
International Chicken Genome Sequencing Consortium, 2004. Sequence and comparative analysis of the chicken genome provide unique perspectives on vertebrate evolution. Nature 432, 695–716. https://doi.org/10.1038/nature03154.
Jarvis, S., Birsa, N., Secrier, M., Fratta, P., Plagnol, V., 2020. A comparison of low read depth QuantSeq 3′ sequencing to total RNA-seq in FUS mutant mice. Front. Genet. 11, 1412. https://doi.org/10.3389/fgene.2020.562445.
Kaneko, N., Kurata, M., Yamamoto, T., Morikawa, S., Masumoto, J., 2019. The role of interleukin-1 in general pathology. Inflamm. Regen. 39, 12. https://doi.org/10.1186/s41232-019-0101-5.
Kanthasamy, A.G., Rangaraju, S., 2020. Molecular signatures of neuroinflammation induced by αSynuclein aggregates in microglial cells. Front. Immunol. 11, 16.
Kempuraj, D., Thangavel, R., Selvakumar, G.P., Zaheer, S., Ahmed, M.E., Raikwar, S.P., Zahoor, H., Saeed, D., Natteru, P.A., Iyer, S., Zaheer, A., 2017. Brain and peripheral atypical inflammatory mediators potentiate neuroinflammation and neurodegeneration. Front. Cell. Neurosci. 11, 216. https://doi.org/10.3389/fncel.2017.00216.
Korpela, J., Kulomaa, M., Tuohimaa, P., Vaheri, A., 1982. Induction of avidin in chickens infected with the acute leukemia virus OK 10. Int. J. Cancer 30, 461–464.
Kumari, R., Fazekas, E.A., Morvai, B., Udvari, E.B., Dóra, F., Zachar, G., Székely, T., Pogány, Á., Dobolyi, Á., 2022. Transcriptomics of parental care in the hypothalamic–septal region of female zebra finch brain. Int. J. Mol. Sci. 23, 2518.
Kunnas, T.A., Wallén, M.J., Kulomaa, M.S., 1993. Induction of chicken avidin and related mRNAs after bacterial infection. Biochim. Biophys. Acta BBA - Gene Struct. Expr. 1216, 441–445. https://doi.org/10.1016/0167-4781(93)90012-3.
Kverková, K., Marhounová, L., Polonyiová, A., Kocourek, M., Zhang, Y., Olkowicz, S., Straková, B., Pavelková, Z., Vodička, R., Frynta, D., Němec, P., 2022. The evolution of brain neuron numbers in amniotes. Proc. Natl. Acad. Sci. USA 119, e2121624119. https://doi.org/10.1073/pnas.2121624119.
Lesur, I., Textoris, J., Loriod, B., Courbon, C., Garcia, S., Leone, M., Nguyen, C., 2010. Gene expression profiles characterize inflammation stages in the acute lung injury in mice. PLoS One 5, e11485.
Li, Y., Xu, Q., Zhang, T., Gao, M., Wang, Q., Han, Z., Shao, Y., Ma, D., Liu, S., 2015. Host avian beta-defensin and toll-like receptor responses of pigeons following infection with pigeon paramyxovirus type 1. Appl. Environ. Microbiol. 81, 6415–6424. https://doi.org/10.1128/AEM.01413-15.
Liu, S., Zhang, S., Sun, Y., Zhou, W., 2021. Transcriptomics changes in the peritoneum of mice with lipopolysaccharide-induced peritonitis. Int. J. Mol. Sci. 22, 13008 https://doi.org/10.3390/ijms222313008.
Liu, Z., Li, W., Geng, L., Sun, L., Wang, Q., Yu, Y., Yan, P., Liang, C., Ren, J., Song, M., 2022. Cross-species metabolomic analysis identifies uridine as a potent regeneration promoting factor. Cell Discov 8, 6.
Lopes, P., Wingfield, J., Bentley, G., 2012. Lipopolysaccharide injection induces rapid decrease of hypothalamic GnRH mRNA and peptide, but does not affect GnIH in zebra finches. Horm. Behav. 62, 173–179.
Lopez-Castejon, G., Brough, D., 2011. Understanding the mechanism of IL-1β secretion. Cytokine Growth Factor Rev. 22, 189–195.
Ma, F., Fuqua, B.K., Hasin, Y., Yukhtman, C., Vulpe, C.D., Lusis, A.J., Pellegrini, M., 2019. A comparison between whole transcript and 3' RNA sequencing methods using Kapa and Lexogen library preparation methods. BMC Genom. 20, 9. https://doi.org/10.1186/s12864-018-5393-3.
Martin, L.B., Han, P., Lewittes, J., Kuhlman, J.R., Klasing, K.C., Wikelski, M., 2006. Phytohemagglutinin-induced skin swelling in birds: histological support for a classic immunoecological technique. Funct. Ecol. 20, 290–299. https://doi.org/10.1111/j.1365-2435.2006.01094.x.
Mayerhofer, R., Fröhlich, E.E., Reichmann, F., Farzi, A., Kogelnik, N., Fröhlich, E., Sattler, W., Holzer, P., 2017. Diverse action of lipoteichoic acid and lipopolysaccharide on neuroinflammation, blood-brain barrier disruption, and anxiety in mice. Brain Behav. Immun. 60, 174–187. https://doi.org/10.1016/j.bbi.2016.10.011.
McDermott, A.M., 2004. Defensins and other antimicrobial peptides at the ocular surface. Ocul. Surf. 2, 229–247. https://doi.org/10.1016/S1542-0124(12)70111-8.
Mello, C.V., 2014. The zebra finch, *Taeniopygia guttata* : an avian model for investigating the neurobiological basis of vocal learning. Cold Spring Harb. Protoc. 2014, emo084574 https://doi.org/10.1101/pdb.emo084574 pdb.
Mesquita, G., Silva, T., Gomes, A.C., Oliveira, P.F., Alves, M.G., Fernandes, R., Almeida, A.A., Moreira, A.C., Gomes, M.S., 2020. H-Ferritin is essential for macrophages' capacity to store or detoxify exogenously added iron. Sci. Rep. 10, 3061. https://doi.org/10.1038/s41598-020-59898-0.
Mills, E.L., Ryan, D.G., Prag, H.A., Dikovskaya, D., Menon, D., Zaslona, Z., Jedrychowski, M.P., Costa, A.S.H., Higgins, M., Hams, E., Szpyt, J., Runtsch, M.C., King, M.S., McGouran, J.F., Fischer, R., Kessler, B.M., McGettrick, A.F., Hughes, M.M., Carroll, R.G., Booty, L.M., Knatko, E.V., Meakin, P.J., Ashford, M.L.J., Modis, L.K., Brunori, G., Sévin, D.C., Fallon, P.G., Caldwell, S.T., Kunji, E.R.S., Chouchani, E.T., Frezza, C., Dinkova-Kostova, A.T., Hartley, R.C., Murphy, M.P., O'Neill, L.A., 2018. Itaconate is an anti-inflammatory metabolite that activates Nrf2 via alkylation of KEAP1. Nature 556, 113–117. https://doi.org/10.1038/nature25986.
Minias, P., Vinkler, M., 2022. Selection balancing at innate immune genes: adaptive polymorphism maintenance in toll-like receptors. Mol. Biol. Evol. 39, msac102 https://doi.org/10.1093/molbev/msac102.
Mishra, I., Knerr, R.M., Stewart, A.A., Payette, W.I., Richter, M.M., Ashley, N.T., 2019. Light at night disrupts diel patterns of cytokine gene expression and endocrine profiles in zebra finch (Taeniopygia guttata). Sci. Rep. 9, 15833.
Moll, P., Ante, M., Seitz, A., Reda, T., 2014. QuantSeq 3′ mRNA sequencing for RNA quantification. Nat. Methods 11, i–iii. https://doi.org/10.1038/nmeth.f.376.
Oliveros, J.C., 2007. VENNY. An Interactive Tool for Comparing Lists with Venn Diagrams. https://bioinfogp.cnb.csic.es/tools/venny/index.html.
Olkowicz, S., Kocourek, M., Lučan, R.K., Porteš, M., Fitch, W.T., Herculano-Houzel, S., Němec, P., 2016. Birds have primate-like numbers of neurons in the forebrain. Proc. Natl. Acad. Sci. USA 113, 7255–7260. https://doi.org/10.1073/pnas.1517131113.
Ozsolak, F., Milos, P.M., 2011. RNA sequencing: advances, challenges and opportunities. Nat. Rev. Genet. 12, 87–98. https://doi.org/10.1038/nrg2934.
Painsipp, E., Herzog, H., Holzer, P., 2010. Evidence from knockout mice that neuropeptide-Y Y2 and Y4 receptor signalling prevents long-term depression-like behaviour caused by immune challenge. J. Psychopharmacol. 24, 1551–1560.
Paus, R., Theoharides, T.C., Arck, P.C., 2006. Neuroimmunoendocrine circuitry of the 'brain-skin connection. Trends Immunol. 27, 32–39.
Pedersen, A.L., Gould, C.J., Saldanha, C.J., 2017. Activation of the peripheral immune system regulates neuronal aromatase in the adult zebra finch brain. Sci. Rep. 7, 10191.
Peralta-Sánchez, J.M., Martín-Vivaldi, M., Martín-Platero, A.M., Martínez-Bueno, M., Oñate, M., Ruiz-Rodríguez, M., Soler, J.J., 2012. Avian life history traits influence eggshell bacterial loads: a comparative analysis. Ibis 154, 725–737. https://doi.org/10.1111/j.1474-919X.2012.01256.x.
Peters, E.M.J., Kuhlmei, A., Tobin, D.J., Müller-Röver, S., Klapp, B.F., Arck, P.C., 2005. Stress exposure modulates peptidergic innervation and degranulates mast cells in murine skin. Brain Behav. Immun. 19, 252–262.
Pfaffl, M.W., 2001. A new mathematical model for relative quantification in real-time RT–PCR. Nucleic Acids Res. 29 e45–e45.
Pfenning, A.R., Hara, E., Whitney, O., Rivas, M.V., Wang, R., Roulhac, P.L., Howard, J.T., Wirthlin, M., Lovell, P.V., Ganapathy, G., 2014. Convergent transcriptional specializations in the brains of humans and song-learning birds. Science 346, 1256846.
Poh, T.Y., Pease, J., Young, J.R., Bumstead, N., Kaiser, P., 2008. Re-evaluation of chicken CXCR1 determines the true gene structure: CXCLi1 (K60) and CXCLi2 (CAF/interleukin-8) are ligands for this receptor. J. Biol. Chem. 283, 16408–16415.
Poole, J., Kitchen, G.B., 2022. Circadian Regulation of Innate Immunity in Animals and Humans and Implications for Human Disease. Presented at the Seminars in Immunopathology. Springer, pp. 183–192.
Poplin, R., Ruano-Rubio, V., DePristo, M.A., Fennell, T.J., Carneiro, M.O., Van der Auwera, G.A., Kling, D.E., Gauthier, L.D., Levy-Moonshine, A., Roazen, D., Shakir, K., Thibault, J., Chandran, S., Whelan, C., Lek, M., Gabriel, S., Daly, M.J., Neale, B., MacArthur, D.G., Banks, E., 2017. Scaling accurate genetic variant discovery to tens of thousands of samples (preprint). Genomics. https://doi.org/10.1101/201178.

Pulido-Salgado, M., Vidal-Taboada, J.M., Barriga, G.G.-D., Solà, C., Saura, J., 2018. RNA-Seq transcriptomic profiling of primary murine microglia treated with LPS or LPS + IFNγ. Sci. Rep. 8, 16096 https://doi.org/10.1038/s41598-018-34412-9.

Ramsköld, D., Luo, S., Wang, Y.-C., Li, R., Deng, Q., Faridani, O.R., Daniels, G.A., Khrebtukova, I., Loring, J.F., Laurent, L.C., Schroth, G.P., Sandberg, R., 2012. Full-length mRNA-Seq from single-cell levels of RNA and individual circulating tumor cells. Nat. Biotechnol. 30, 777–782. https://doi.org/10.1038/nbt.2282.

Rankine, E.L., Hughes, P.M., Botham, M.S., Perry, V.H., Felton, L.M., 2006. Brain cytokine synthesis induced by an intraparenchymal injection of LPS is reduced in MCP-1-deficient mice prior to leucocyte recruitment. Eur. J. Neurosci. 24, 77–86. https://doi.org/10.1111/j.1460-9568.2006.04891.x.

Raudvere, U., Kolberg, L., Kuzmin, I., Arak, T., Adler, P., Peterson, H., Vilo, J., 2019. g: Profiler: a web server for functional enrichment analysis and conversions of gene lists (2019 update). Nucleic Acids Res. 47, W191–W198. https://doi.org/10.1093/nar/gkz369.

Romanov, M.N., Farré, M., Lithgow, P.E., Fowler, K.E., Skinner, B.M., O'Connor, R., Fonseka, G., Backström, N., Matsuda, Y., Nishida, C., Houde, P., Jarvis, E.D., Ellegren, H., Burt, D.W., Larkin, D.M., Griffin, D.K., 2014. Reconstruction of gross avian genome structure, organization and evolution suggests that the chicken lineage most closely resembles the dinosaur avian ancestor. BMC Genom. 15, 1060. https://doi.org/10.1186/1471-2164-15-1060.

Russell, J.J., Theriot, J.A., Sood, P., Marshall, W.F., Landweber, L.F., Fritz-Laylin, L., Polka, J.K., Oliferenko, S., Gerbich, T., Gladfelter, A., Umen, J., Bezanilla, M., Lancaster, M.A., He, S., Gibson, M.C., Goldstein, B., Tanaka, E.M., Hu, C.-K., Brunet, A., 2017. Non-model model organisms. BMC Biol. 15 (55) https://doi.org/10.1186/s12915-017-0391-5 s12915-017-0391–5.

Santiago-Quesada, F., Albano, N., Castillo-Guerrero, J.A., Fernández, G., González-Medina, E., Sánchez-Guzmán, J.M., 2015. Secondary phytohaemagglutinin (PHA) swelling response is a good indicator of T-cell-mediated immunity in free-living birds. Ibis 157, 767–773.

Satam, H., Joshi, K., Mangrolia, U., Waghoo, S., Zaidi, G., Rawool, S., Thakare, R.P., Banday, S., Mishra, A.K., Das, G., 2023. Next-generation sequencing technology: current trends and advancements. Biology 12, 997.

Scalf, C.S., Chariker, J.H., Rouchka, E.C., Ashley, N.T., 2019. Transcriptomic analysis of immune response to bacterial lipopolysaccharide in zebra finch (*Taeniopygia guttata*). BMC Genom. 20, 647. https://doi.org/10.1186/s12864-019-6016-3.

Scott, M.G., Hancock, R.E., 2000. Cationic antimicrobial peptides and their multifunctional role in the immune system. Crit. Rev. Immunol. 20, 407–31.

Seal, S., Dharmarajan, G., Khan, I., 2021. Evolution of pathogen tolerance and emerging infections: a missing experimental paradigm. Elife 10, e68874. https://doi.org/10.7554/eLife.68874.

Seok, J., Warren, H.S., Cuenca, A.G., Mindrinos, M.N., Baker, H.V., Xu, W., Richards, D. R., McDonald-Smith, G.P., Gao, H., Hennessy, L., 2013. Genomic responses in mouse models poorly mimic human inflammatory diseases. Proc. Natl. Acad. Sci. USA 110, 3507–3512.

Shaftel, S.S., Griffin, W.S.T., O'Banion, M.K., 2008. The role of interleukin-1 in neuroinflammation and Alzheimer disease: an evolving perspective. J. Neuroinflammation 5, 7. https://doi.org/10.1186/1742-2094-5-7.

Shahzad, A., Knapp, M., Lang, I., Köhler, G., 2010. Interleukin 8 (IL-8)-a universal biomarker? Int. Arch. Med. 3, 1–4.

Shi, S., Blumenthal, A., Hickey, C.M., Gandotra, S., Levy, D., Ehrt, S., 2005. Expression of many immunologically important genes in Mycobacterium tuberculosis-infected macrophages is independent of both TLR2 and TLR4 but dependent on IFN-αβ receptor and STAT11. J. Immunol. 175, 3318–3328. https://doi.org/10.4049/jimmunol.175.5.3318.

Sköld-Chiriac, S., Nord, A., Nilsson, J.-Å., Hasselquist, D., 2014. Physiological and behavioral responses to an acute-phase response in zebra finches: immediate and short-term effects. Physiol. Biochem. Zool. 87, 288–298.

Smedley, D., Haider, S., Durinck, S., Pandini, L., Provero, P., Allen, J., Arnaiz, O., Awedh, M.H., Baldock, R., Barbiera, G., Bardou, P., Beck, T., Blake, A., Bonierbale, M., Brookes, A.J., Bucci, G., Buetti, I., Burge, S., Cabau, C., Carlson, J.W., Chelala, C., Chrysostomou, C., Cittaro, D., Collin, O., Cordova, R., Cutts, R.J., Dassi, E., Genova, A.D., Djari, A., Esposito, A., Estrella, H., Eyras, E., Fernandez-Banet, J., Forbes, S., Free, R.C., Fujisawa, T., Gadaleta, E., Garcia-Manteiga, J.M., Goodstein, D., Gray, K., Guerra-Assunção, J.A., Haggarty, B., Han, D.-J., Han, B.W., Harris, T., Harshbarger, J., Hastings, R.K., Hayes, R.D., Hoede, C., Hu, S., Hu, Z.-L., Hutchins, L., Kan, Z., Kawaji, H., Keliet, A., Kerhornou, A., Kim, S., Kinsella, R., Klopp, C., Kong, L., Lawson, D., Lazarevic, D., Lee, J.-H., Letellier, T., Li, C.-Y., Lio, P., Liu, C.-J., Luo, J., Maass, A., Mariette, J., Maurel, T., Merella, S., Mohamed, A.M., Moreews, F., Nabihoudine, I., Ndegwa, N., Noirot, C., Perez-Llamas, C., Primig, M., Quattrone, A., Quesneville, H., Rambaldi, D., Reecy, J., Riba, M., Rosanoff, S., Saddiq, A.A., Salas, E., Sallou, O., Shepherd, R., Simon, R., Sperling, L., Spooner, W., Staines, D.M., Steinbach, D., Stone, K., Stupka, E., Teague, J.W., Dayem Ullah, A.Z., Wang, J., Ware, D., Wong-Erasmus, M., Youens-Clark, K., Zadissa, A., Zhang, S.-J., Kasprzyk, A., 2015. The BioMart community portal: an innovative alternative to large, centralized data repositories. Nucleic Acids Res. 43, W589–W598. https://doi.org/10.1093/nar/gkv350.

So, S.W., Fleming, K.M., Duffy, C.M., Nixon, J.P., Bernlohr, D.A., Butterick, T.A., 2022. Microglial FABP4-UCP2 Axis modulates neuroinflammation and cognitive decline in obese mice. Int. J. Mol. Sci. 23, 4354. https://doi.org/10.3390/ijms23084354.

Söllner, J.F., Leparc, G., Hildebrandt, T., Klein, H., Thomas, L., Stupka, E., Simon, E., 2017. An RNA-Seq atlas of gene expression in mouse and rat normal tissues. Sci. Data 4, 170185. https://doi.org/10.1038/sdata.2017.185.

Song, X., Li, M., Wu, W., Dang, W., Gao, Y., Bian, R., Bao, R., Hu, Y., Hong, D., Gu, J., Liu, Y., 2020. Regulation of BMP2K in AP2M1-mediated EGFR internalization during the development of gallbladder cancer. Signal Transduct. Targeted Ther. 5, 154. https://doi.org/10.1038/s41392-020-00250-3.

Sousa, C.S., Power, D.M., Guerreiro, P.M., Louro, B., Chen, L., Canário, A.V., 2022. Transcriptomic down-regulation of immune system components in barrier and hematopoietic tissues after lipopolysaccharide injection in antarctic notothenia coriiceps. Fishes 7, 171.

Spierings, M.J., ten Cate, C., 2016. Zebra finches as a model species to understand the roots of rhythm. Front. Neurosci. 10 https://doi.org/10.3389/fnins.2016.00345.

Sulakhiya, K., Keshavlal, G.P., Bezbaruah, B.B., Dwivedi, S., Gurjar, S.S., Munde, N., Jangra, A., Lahkar, M., Gogoi, R., 2016. Lipopolysaccharide induced anxiety- and depressive-like behaviour in mice are prevented by chronic pre-treatment of esculetin. Neurosci. Lett. 611, 106–111. https://doi.org/10.1016/j.neulet.2015.11.031.

Team, R.C., 2013. R: A Language and Environment for Statistical Computing.

Terenina, E., Sautron, V., Ydier, C., Bazovkina, D., Sevin-Pujol, A., Gress, L., Lippi, Y., Naylies, C., Billon, Y., Liaubet, L., Mormede, P., Villa-Vialaneix, N., 2017. Time course study of the response to LPS targeting the pig immune gene networks. BMC Genom. 18, 988. https://doi.org/10.1186/s12864-017-4363-5.

Těšický, M., Velová, H., Novotný, M., Kreisinger, J., Beneš, V., Vinkler, M., 2020. Positive selection and convergent evolution shape molecular phenotypic traits of innate immunity receptors in tits (Paridae). Mol. Ecol. 29, 3056–3070.

The UniProt Consortium, Bateman, A., Martin, M.-J., Orchard, S., Magrane, M., Agivetova, R., Ahmad, S., Alpi, E., Bowler-Barnett, E.H., Britto, R., Bursteinas, B., Bye-A-Jee, H., Coetzee, R., Cukura, A., Da Silva, A., Denny, P., Dogan, T., Ebenezer, T., Fan, J., Castro, L.G., Garmiri, P., Georghiou, G., Gonzales, L., Hatton-Ellis, E., Hussein, A., Ignatchenko, A., Insana, G., Ishtiaq, R., Jokinen, P., Joshi, V., Jyothi, D., Lock, A., Lopez, R., Luciani, A., Luo, J., Lussi, Y., MacDougall, A., Madeira, F., Mahmoudy, M., Menchi, M., Mishra, A., Moulang, K., Nightingale, A., Oliveira, C.S., Pundir, S., Qi, G., Raj, S., Rice, D., Lopez, M.R., Saidi, R., Sampson, J., Sawford, T., Speretta, E., Turner, E., Tyagi, N., Vasudev, P., Volynkin, V., Warner, K., Watkins, X., Zaru, R., Zellner, H., Bridge, A., Poux, S., Redaschi, N., Aimo, L., Argoud-Puy, G., Auchincloss, A., Axelsen, K., Bansal, P., Baratin, D., Blatter, M.-C., Bolleman, J., Boutet, E., Breuza, L., Casals-Casas, C., de Castro, E., Echioukh, K.C., Coudert, E., Cuche, B., Doche, M., Dornevil, D., Estreicher, A., Famiglietti, M.L., Feuermann, M., Gasteiger, E., Gehant, S., Gerritsen, V., Gos, A., Gruaz-Gumowski, N., Hinz, U., Hulo, C., Hyka-Nouspikel, N., Jungo, F., Keller, G., Kerhornou, A., Lara, V., Le Mercier, P., Lieberherr, D., Lombardot, T., Martin, X., Masson, P., Morgat, A., Neto, T.B., Paesano, S., Pedruzzi, I., Pilbout, S., Pourcel, L., Pozzato, M., Pruess, M., Rivoire, C., Sigrist, C., Sonesson, K., Stutz, A., Sundaram, S., Tognolli, M., Verbregue, L., Wu, C.H., Arighi, C.N., Arminski, L., Chen, C., Chen, Y., Garavelli, J.S., Huang, H., Laiho, K., McGarvey, P., Natale, D.A., Ross, K., Vinayaka, C.R., Wang, Q., Wang, Y., Yeh, L.-S., Zhang, J., Ruch, P., Teodoro, D., 2021. UniProt: the universal protein knowledgebase in 2021. Nucleic Acids Res 49, D480–D489. https://doi.org/10.1093/nar/gkaa1100.

Vance, D.D., 2014. Dynamic gene expression profile changes in synovial fluid following meniscal injury; osteoarthritis (OA) markers found. J. Exerc. Sports Orthop. 1 https://doi.org/10.15226/2374-6904/1/3/00115.

Vinkler, M., Bryjová, A., Albrecht, T., Bryja, J., 2009. Identification of the first Toll-like receptor gene in passerine birds: TLR4 orthologue in zebra finch (*Taeniopygia guttata*). Tissue Antigens 74, 32–41. https://doi.org/10.1111/j.1399-0039.2009.01273.x.

Vinkler, M., Bainová, H., Albrecht, T., 2010. Functional analysis of the skin-swelling response to phytohaemagglutinin. Funct. Ecol. 24, 1081–1086.

Vinkler, M., Schnitzer, J., Munclinger, P., Albrecht, T., 2012. Phytohaemagglutinin skin-swelling test in scarlet rosefinch males: low-quality birds respond more strongly. Anim. Behav. 83, 17–23.

Vinkler, M., Leon, A.E., Kirkpatrick, L., Dalloul, R.A., Hawley, D.M., 2018. Differing house finch cytokine expression responses to original and evolved isolates of mycoplasma gallisepticum. Front. Immunol. 9, 13. https://doi.org/10.3389/fimmu.2018.00013.

Vinkler, M., Adelman, J.S., Ardia, D.R., 2022. Chapter 20 - evolutionary and ecological immunology. In: Kaspers, B., Schat, K.A., Göbel, T.W., Vervelde, L. (Eds.), Avian Immunology, third ed. Academic Press, Boston, pp. 519–557. https://doi.org/10.1016/B978-0-12-818708-1.00008-7.

n.d. Vinkler, M., Fiddaman, S.R., Těšický, M., O'Connor, E.A., Savage, A.E., Lenz, T.L., Smith, A.L., Kaufman, J., Bolnick, D.I., Davies, C.S., Dedić, N., Flies, A.S., Gomez Samblás, M.M., Henschen, A.E., Novák, K., Palomar, G., Raven, N., Samaké, K., Slade, J., Kuttiyarthu Veetil, N., Voukali, E., Höglund, J., Richardson, D.S, Westerdahl, H., 2023. Understanding the evolution of immune genes in jawed vertebrates J. Evol. Biol. 36 (6), 847–873 https://doi.org/10.1111/jeb.14181.

Vo, T.T.M., Nguyen, T.V., Amoroso, G., Ventura, T., Elizur, A., 2021. Deploying new generation sequencing for the study of flesh color depletion in Atlantic Salmon (Salmo salar). BMC Genom. 22, 545. https://doi.org/10.1186/s12864-021-07884-9.

Wang, Z., Gerstein, M., Snyder, M., 2009. RNA-Seq: a revolutionary tool for transcriptomics. Nat. Rev. Genet. 10, 57–63. https://doi.org/10.1038/nrg2484.

Warren, W.C., Clayton, D.F., Ellegren, H., Arnold, A.P., Hillier, L.W., Künstner, A., Searle, S., White, S., Vilella, A.J., Fairley, S., Heger, A., Kong, L., Ponting, C.P., Jarvis, E.D., Mello, C.V., Minx, P., Lovell, P., Velho, T.A.F., Ferris, M., Balakrishnan, C.N., Sinha, S., Blatti, C., London, S.E., Li, Y., Lin, Y.-C., George, J., Sweedler, J., Southey, B., Gunaratne, P., Watson, M., Nam, K., Backström, N., Smeds, L., Nabholz, B., Itoh, Y., Whitney, O., Pfenning, A.R., Howard, J., Völker, M., Skinner, B.M., Griffin, D.K., Ye, L., McLaren, W.M., Flicek, P., Quesada, V., Velasco, G., Lopez-Otin, C., Puente, X.S., Olender, T., Lancet, D., Smit, A.F.A., Hubley, R., Konkel, M.K., Walker, J.A., Batzer, M.A., Gu, W., Pollock, D.D., Chen, L., Cheng, Z., Eichler, E.E., Stapley, J., Slate, J., Ekblom, R., Birkhead, T., Burke, T., Burt, D., Scharff, C., Adam, I., Richard, H., Sultan, M., Soldatov, A., Lehrach, H.,

Edwards, S.V., Yang, S.-P., Li, X., Graves, T., Fulton, L., Nelson, J., Chinwalla, A., Hou, S., Mardis, E.R., Wilson, R.K., 2010. The genome of a songbird. Nature 464, 757–762. https://doi.org/10.1038/nature08819.

Wegmann, M., Voegeli, B., Richner, H., 2015. Parasites suppress immune-enhancing effect of methionine in nestling great tits. Oecologia 177, 213–221. https://doi.org/10.1007/s00442-014-3138-9.

Wu, R., Kang, R., Tang, D., 2022. Mitochondrial ACOD1/IRG1 in Infection and Sterile Inflammation. J. Intensive Med. 2, 78–88. https://doi.org/10.1016/j.jointm.2022.01.001.

Yoshino, Y., Roy, B., Kumar, N., Shahid Mukhtar, M., Dwivedi, Y., 2021. Molecular pathology associated with altered synaptic transcriptome in the dorsolateral prefrontal cortex of depressed subjects. Transl. Psychiatry 11, 73. https://doi.org/10.1038/s41398-020-01159-9.

Zeng, J., Wang, Y., Luo, Z., Chang, L.-C., Yoo, J.S., Yan, H., Choi, Y., Xie, X., Deverman, B.E., Gradinaru, V., Gupton, S.L., Zlokovic, B.V., Zhao, Z., Jung, J.U., 2019. TRIM9-Mediated resolution of neuroinflammation confers neuroprotection upon ischemic stroke in mice. Cell Rep. 27, 549–560.e6. https://doi.org/10.1016/j.celrep.2018.12.055.

Zerega, B., Camardella, L., Cermelli, S., Sala, R., Cancedda, R., Descalzi Cancedda, F., 2001. Avidin expression during chick chondrocyte and myoblast development in vitro and in vivo: regulation of cell proliferation. J. Cell Sci. 114, 1473–1482.

Zheng, X., Levine, D., Shen, J., Gogarten, S.M., Laurie, C., Weir, B.S., 2012. A high-performance computing toolset for relatedness and principal component analysis of SNP data. Bioinformatics 28, 3326–3328. https://doi.org/10.1093/bioinformatics/bts606.

Zheng, D., Liwinski, T., Elinav, E., 2020. Interaction between microbiota and immunity in health and disease. Cell Res. 30, 492–506. https://doi.org/10.1038/s41422-020-0332-7.